

16th CIRP Conference on Intelligent Computation in Manufacturing Engineering, CIRP ICME '22, Italy

# Marker-free identification of turned, ground and deep rolled workpieces using wavelet transformation

Bernd Breidenstein<sup>a</sup>, Marcel Wichmann<sup>a</sup>, Hendrik Voelker<sup>a,\*</sup>

<sup>a</sup>*Institute of Production Engineering and Machine Tools Leibniz Universität Hannover, An der Universität 2, 30823 Garbsen, Germany*

\* Corresponding author. Tel.: +49 511 762 8078; E-mail address: [voelker@ifw.uni-hannover.de](mailto:voelker@ifw.uni-hannover.de)

## Abstract

This paper presents a marker-free component identification of cylindrical workpieces produced by the manufacturing processes turning, grinding and deep rolling. The position of unique features from a 2-D profile in the 3-D frequency is detected for identification. Therefore, this work presents an approach using an industrial camera for surface measuring to clearly identify individual cylindrical components. In addition, wear tests are carried out to investigate the method's robustness. The results after the wear tests indicate a false positive rate of  $10^{-20}$ .

© 2023 The Authors. Published by Elsevier B.V.

This is an open access article under the CC BY-NC-ND license (<https://creativecommons.org/licenses/by-nc-nd/4.0>)

Peer-review under responsibility of the scientific committee of the 16th CIRP Conference on Intelligent Computation in Manufacturing Engineering

*Keywords:* Identification; Surface analysis; Wavelet transformation

## 1. Introduction

Complaints due to faulty production or counterfeit products from third parties are a significant problem in German mechanical and plant engineering. The monetary damage caused by counterfeits alone amounts to 7.6 billion euros in 2020 for German companies [1]. Customer claims could be one of the consequences of the complaints. To avoid compensation payments, the manufacturer is obliged to ensure that the product was delivered in a fault-free condition. In the case of counterfeits, the manufacturer must prove that he did not produce the component. Therefore, it is necessary to trace the products throughout their lifecycle from production to use. For the ability to trace parts, a unique marking for identification is needed. Currently, companies use different active markings, ranging from a QR code to a serial number. However, the disadvantage of active marking is an additional application step at the end of the process chain. In addition, the shape or functional area of the component can make active marking difficult. For this reason, an efficient and cross-industry

method for component marking is needed that can be applied to any component shape.

Passive markings can realize an identification system with these requirements. One approach is the marker-free identification of components. For the ability to identify parts without marking, it is necessary to extract properties of the components that are different, even if the primary conditions of the manufacturing are the same. Possible features are the surface's shape, color, or texture [2]. One method that is already applied in industry is the "Laser Surface Authentication" method (LSA) by Cowburn [3]. Here, a laser beam diffusely reflected by the packaging creates interference patterns, so-called speckles. By evaluating these speckles, the method can determine the authenticity of the packaging. Due to the unique fiber structure of packaging materials, this identification process cannot be imitated. The method is limited to paper and plastic surfaces. Implementing the LSA method on metallic materials to identify machined components is not yet known.

However, machined components also have unique surface features, which are created during the machining process. For example, the tool's hardness or the machine's vibrations can

generate these features. Even if the general conditions during machining remain the same, microscopic differences occur in the surface. The method of the Fraunhofer Institute for Physical Measurement Techniques (IPM), for example, uses these unique features of the component surface [4]. IPM's fingerprint method uses high-resolution cameras to extract the distinctive points from the surface. The arrangement of these points among each is so unique that it is referred to as fingerprint. The fingerprint is stored in a database in the form of a bit sequence [4]. This method directly identifies a component or product. A similar approach is followed by the method of the Institute for Information Processing (TNT) and the Institute of Production Engineering and Machine Tools (IFW) of the Leibniz University Hannover. Here the method extracts the unique features using an optical or tactile measurement of the surface [5]. Features in the frequency range are then extracted from a 2-D profile of the 3-D measurement using the continuous wavelet transformation. Since the features can be present in different directions in the surface, the profile position of the 2-D profile is decisive for the feature extraction [5].

To identify components using the method of marker-free component identification, it is necessary to understand how the surface is produced. With the knowledge of the surface composition, it is possible to determine the correct profile position, which makes identification possible in the first place. Within the Collaborative Research Centre 653, the method was applied to components produced with the manufacturing process of surface grinding [6]. In this work, the method will be applied to different manufacturing processes that produce a cylindrical workpiece. For this purpose, materials are machined with turning and a combination of turning and deep rolling. The surface in the grinding process is created by the impact of the abrasive grain on the material. The grain engagement on the surface occurs with the cutting direction. In the Collaborative Research Centre 653, it was shown that identifying the components perpendicular to the cutting direction during grinding achieves a high degree of identification reliability [7]. This means that several grain intersections in the surface can be used for identification, which forms the unique surface due to the statistical arrangement of the abrasive grains. Similar behavior also occurs with cylindrical grinding. The grain interferences also occur with the cutting direction, so an algorithm adaptation is unnecessary. In turning, the tool cutting edge is guided with the feed over a rotating component [8]. The feed rate defines the kinematic roughness of the surface. The stochastic features of the surface are also present in feed direction. Here, as in grinding, the stochastic and kinematic components of the surface are present in the same direction. Therefore, a possible profile could be selected for the identification method in this direction [10, 9].

In deep rolling, a rolling element is guided with a feed rate over a rotating component. As in turning, the feed rate defines the surface roughness in deep rolling, so the highest identification probability can be expected when the method is applied in feed direction. However, in deep rolling, there is only a material deformation, but no separation of the material [11, 12]. Thus, within the scope of this work, an investigation is necessary to identify the direction of the stochastic features

in the surface. Therefore this paper proposes and implements the following solutions:

- Qualification of different manufacturing processes based on their surface composition
- Adaptation of the parameters of the identification algorithm for the investigated manufacturing processes
- Influence of surface changes from a mechanical wear test on the identification reliability
- Research of a measurement routine for reliable identification of cylindrical components.

## 2. Marker-free identification method

Figure 1 shows the flowchart of the identification method. By this the method uses the continuous wavelet transformation (CWT) to extract the features from an optical or tactile measurement [5]. This is done by using a profile section from the measurement, which is converted into a local spectrum via the CWT. In order to remove measurement errors, several profiles lying parallel to each other are averaged. When considering the number of profiles for averaging, it should be noted that as the number of profiles increases, the uniqueness of the fingerprint decreases. Filtering removes more high-frequency information, such as tool uniqueness and thus, precise identification is not possible. If too few profiles are used, the identification result may be falsified due to measurement errors, leading to a false identification. In their work on ground surfaces, Dragon et al. have shown that the calculation of the mean value from 60 profiles shows the most robust identification [5]. From the result of the CWT the non-maxima suppression extracts local maxima, which are defined as features. For this purpose, a threshold value  $t_{nms}$  is set that specifies the minimum correlation that a feature must fulfill. This threshold value must be adjusted individually for each production process.

A feature is defined as a coordinate of frequency  $f$  and position  $x$ . All features are defined as a region to prevent a surface feature from being represented twice [6]. The region is

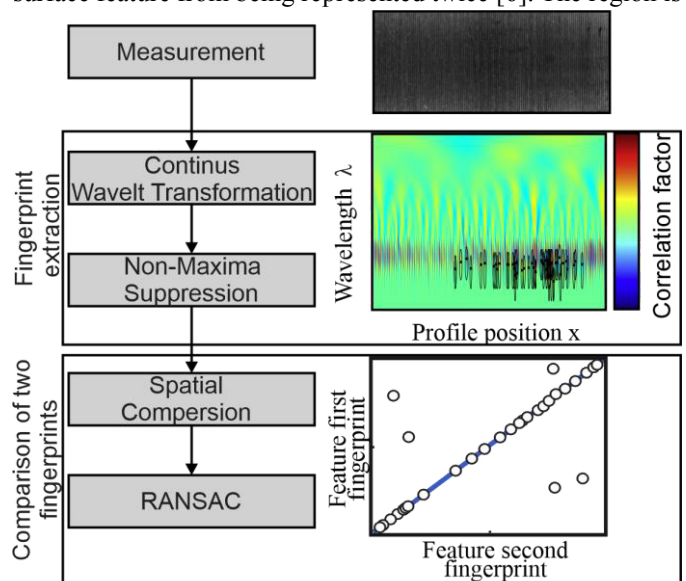


Fig. 1. Functionality of the marker-free component identification from the Collaborative Research Centre 653.

defined as an ellipse, with the size of the ellipse depending on the frequency of the feature. If a feature with a smaller correlation factor is located in the region of another feature, it will be removed by the algorithm. The available fingerprints from two independent measurements are compared to identify a component. For this purpose, the features are checked for their spatial similarity before the remaining features are compared for their statistical correspondence using the RANSAC algorithm [13]. In the Collaborative Research Centre 653, the method was successfully validated experimentally using 500 ground workpieces. It was found that 20 matching features are enough to ensure a false-positive rate of  $10^{-20}$  [6].

Dragon et al. derived a probability model to determine the false-positive rate that a number of matching features achieves [5]. For this purpose, the model uses the probability that outliers occur when comparing two fingerprints. Outliers can occur after the spatial comparison of two features or after the comparison with the RANSAC algorithm. The likelihood of outliers is determined by comparing two profiles of a component at a distance of 1 mm from each other. The stochastic features of a machined surface are so unique that even the smallest deviations no longer allow identification. After determining the probability of outliers, Dragon et al. use the binomial distribution to calculate the probability that exactly two outliers meet the outlier criteria [5]. The probability model can assign a false-positive rate to each number of matching features. A component must now exceed the number of features for a selected false positive rate for successful identification.

### 3. Experimental setup

In order to validate the marker-free component identification for the manufacturing processes deep rolling, cylindrical grinding and turning, 120 samples were produced and examined in this work. Overall 20 samples for grinding, 20 samples for deep rolling as well as 80 samples for turning were used. For turning, the process parameters were kept constant in half of the experiments and varied in the other half. This makes it possible to investigate different surface characteristics and to evaluate the uniqueness by the validation of surfaces produced by the same parameters. The topography of the manufactured workpieces is measured using the industrial camera Basler acA5472-17um from the company Basler AG. The industrial camera is advantageous for cost, measuring time, and integration into the production process. The camera from Basler AG is a monochrome area scan camera, which is used in most applications for image acquisition. The sensor used in the camera has a large matrix of image pixels so that an ordinary two-dimensional image can be produced with one exposure cycle. The camera has a resolution of  $5472 \times 3648$  pixels, with a pixel size of  $2.4 \mu\text{m}$ . A LM series lens from Kowa is used for the focusing of the object. This results in a working distance of 200 mm and a pixel size of  $3.1 \mu\text{m}$ . Compared to the precise laboratory camera, the disadvantage of the industrial camera is the sensitivity to external interfering factors (e.g., light conditions) with the associated higher measuring reliability. LED dark field ring illumination captures surface structures for component identification. This light has already been qualified

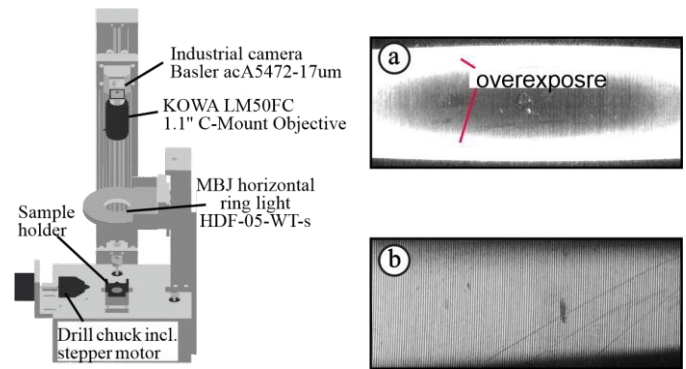


Fig. 2. Measurement set-up for the investigations with two different exposure sources.

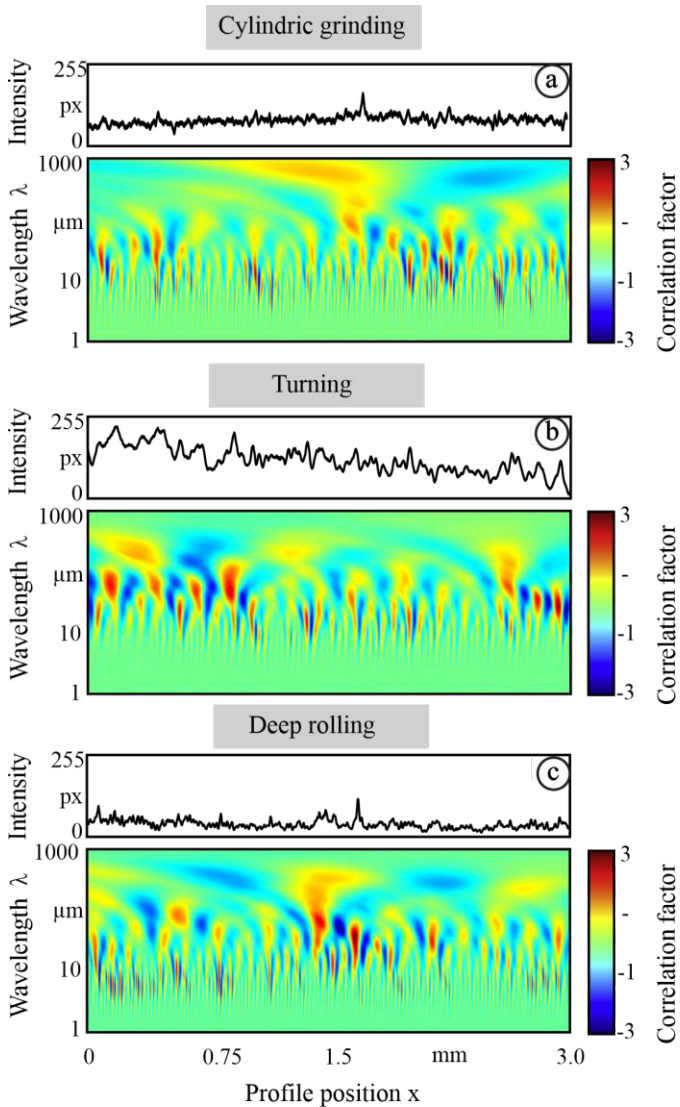
for flat samples and is now to be transferred for use on cylindrical samples. The light is shone flat onto the sample to reflect irregularities, scratches, or rough grooves onto the camera.

Figure 2 shows the experimental setup of this work on the left. The camera and the light source are controlled via a linear axis to adjust the focus range for different component heights. In order to identify a component with the marker-free component identification method, it is necessary to measure the same position of the fingerprint on the workpiece. Due to the high proportion of stochastic parts on the surface, even a slight deviation of the position leads to a non-existent identification [5]. For flat surfaces, edges, corners, or holes can be used to orient a measurement routine. Finding the same measuring position with cylindrical samples is a more significant problem. For initial tests, a holder was constructed on which the rotating workpieces can be precisely placed with a hole. By this, the marker-free component identification can be validated in the first series of tests. However, this cannot be used for later implementation in industry. Therefore, the experimental set-up is expanded to include a stepper motor with a drill chuck, which can be used to rotate the cylindrical workpieces. By stitching several measurements together, the surface area can be recorded. Thus, only a single location from the surface can be found and compared in a second measurement.

On the right side of Figure 2 there are two images of the same cylindrical samples with different exposures. The image in Figure 2a was taken with ring illumination. The distinctive features such as scratches, contamination or surface damage are visible in the image. However, there is over-illumination at the edges of the workpiece and thus no uniform exposure can take place. Therefore, a different illumination setting was used in Figure 2b. Here, a uniform exposure was succeeded by using back light, which exposes the light from one side. The feed grooves are well represented by the change from light to dark. However, this results in a loss of individual surface features. Therefore, the ring illumination is used in this work. For the identification a profile cut between the overexposure is set and compared.

### 4. Experimental Results

Figure 3 shows the resulting surfaces after cylindrical grinding, turning and deep rolling with their respective fingerprint. The surface is measured with the industrial camera. From the image, a profile section of 1000 px is extracted. With a resolution of 3.1 μm that means a profile length of 3.1 mm. For each extracted profile, the continuous wavelet transformations are taken. From Dragon et al., it is known that the profile section for grinding must be orthogonal to the cutting direction [5]. In the case of cylindrical grinding, this means that the profile section is in feed direction. For all three processes, the wavelength is set from 1 μm to 1000 μm to get a complete characterization of the surface. The scaling of the wavelength depends on the resolution of the measuring equipment. For example, feed grooves of 310 μm measured at a resolution of 3.1 μm result in a wavelength of 100 μm. It is thus clear that the measuring resolution must be considered for the settings of the wavelengths for the CWT. Dragon et al. determined λ<sub>1</sub> over the profile length, including the measuring resolution. However, λ<sub>0</sub> was determined in their work via the grain size [5]. The grain size is an exceptional value for



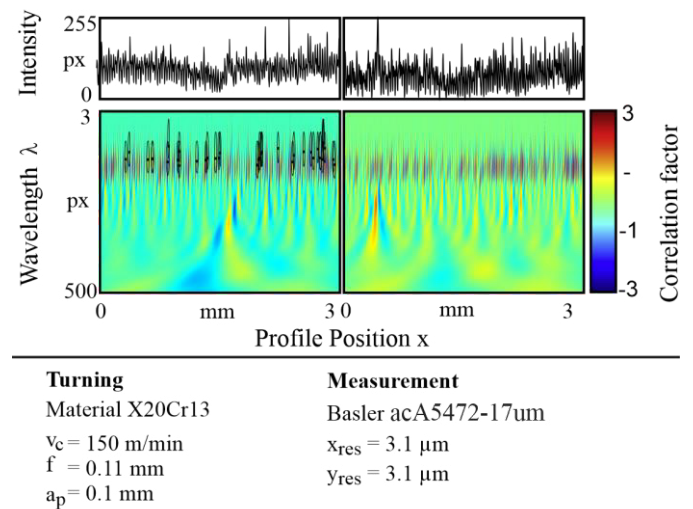
VI/111437 ©IFW

Fig. 3. Surface characterisation of the three manufacturing process with continuous wavelet transformation.

grinding and is not applicable to all processes. In the CWT, no surface characteristics that are smaller than the measurement resolution can be displayed. Therefore, this work will adjust λ<sub>0</sub> to the same value as the measurement resolution. This results in the following wavelength λ<sub>0</sub> = x<sub>res</sub> to λ<sub>1</sub> = s<sub>x</sub>/2 for the three processes, where s<sub>x</sub> is the profile length.

There is still no specific profile cross-section in the literature for marker-free component identification for turning and deep rolling. However, it is known from the literature that the stochastic features are present for turning in feed direction [9, 10]. In the CWT of the turning profiles, the feed grooves can be seen in the high wavelength region. Below the feed grooves, peaks can be seen, which change slightly with tool wear. In summary, all features are present, which is why the profile cut will be selected in feed direction of the process. Deep rolling is a process that is applied to surfaces produced by turning. By this, deep rolling does not remove material but has a forming effect. Depending on the material and the selected rolling pressure, the stochastic features from turning are removed in the newly created surface. The feed grooves also shift in the process, depending on the feed rate selected for deep rolling. As in turning, the grooves can be seen in a profile cross-section in feed direction. The peaks below the feed grooves have decreased because of the plastic deformation. However, the profile cut must also be selected in feed direction.

In order to validate the profile sections, the following takes a closer look at the difference between the two fingerprints. Therefore, two profile sections from the same turned surface are compared, that are 1.5 mm apart. In the work of Dragon et al., it could be proven that by measuring with laboratory equipment the distance of 1 mm is sufficient to no longer achieve a clear identification. Figure 4 shows the two fingerprints of the different profiles manufactured by turning. The profile cross-section is like defined beforehand parallel to the feed direction. It can be noted that the feed grooves are identical in the higher wavelength range. The differences between the two profiles are shown in the lower wavelength region. The imprint of the tool and vibrations on the system cause these characteristics in the surface. Due to wear and the stochastic composition of the turning tool, there are unique



VI/111439 ©IFW

Fig. 4. Comparison of two profiles in distance of 1.5 mm.

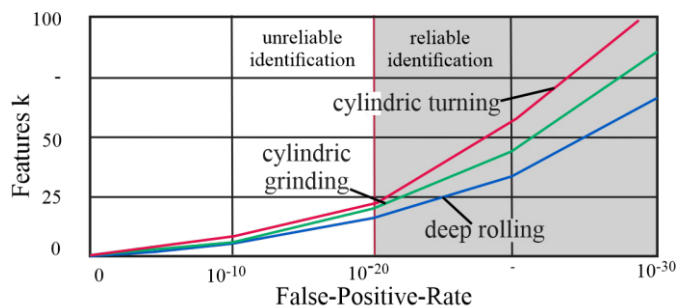
differences in the surface that can be recognized as features. An identification is still possible, however, if the profiles are 1.5 mm apart, only 28 features out of a possible number of 38,190 can be recognized.

With the knowledge of the surface composition, the associated profile cut and the uniqueness of the selected profile cut, the next step is to optimize the parameters of the algorithm. The two threshold values of the non-maxima suppression and the spatial comparison are decisive for the identification reliability. These values must currently be adjusted for each production process and each combination of process parameters. This leads to a significant effort in the later implementation in the industry. Therefore, an automated determination for the threshold value of the non-maxima suppression is implemented in the following. For this, the distribution of the correlation from the CWT is used. The threshold value can then be determined via the percentage distribution by specifying a minimum value to be exceeded. The study in Table 1 shows that a value of 85 percent is preferable, as it allows an identification of each sample and there are no false positives.

Table 1. Determination of the threshold for non-maxima suppression.

Threshold for the non-maxima suppression	Correct identification	False-Positive Identification
70 %	120	10
80%	120	5
85 %	120	0
90 %	110	0

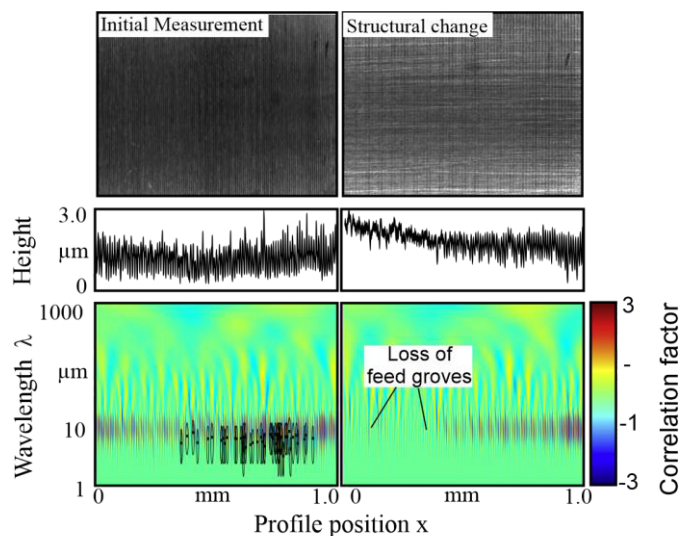
After the profile section and the algorithm parameters have been adjusted, the next step is to determine the identification reliability of the individual processes. For this purpose, the probability model of Dragon et al. is used [5]. According to them the profile sections to be compared should be 1 mm apart. However, the previous results show that with the industrial camera the distance of 1.5 mm between two profiles still allows identification, so the distance of 3.1 mm and thus 1000 pixels is chosen for these investigations. Figure 5 shows the false-positive rates for the investigated process kinematics, which are almost identical. However, turning and grinding show



Turning	Grinding	Deep rolling	Measurement
$v_c = \text{var.}$	$v_c = \text{var.}$	$v_c = \text{var.}$	Basler acA5472-17um
$f = \text{var.}$	$v_f = \text{var.}$	$f = \text{var.}$	$x_{\text{res}} = 3.1 \mu\text{m}$
$a_p = \text{var.}$	$a_p = \text{var.}$		$y_{\text{res}} = 3.1 \mu\text{m}$

VI/111438 ©IFW

Fig. 5. Identification reliability for the machining processes turning, deep rolling and cylindrical grinding.



Turning	Measurement
Material X20Cr13	Basler acA5472-17um
$v_c = 150 \text{ m/min}$	$x_{\text{res}} = 3.1 \mu\text{m}$
$f = 0.11 \text{ mm}$	$y_{\text{res}} = 3.1 \mu\text{m}$
$a_p = 0.1 \text{ mm}$	

VI/111439 ©IFW

Fig. 6. Influence of surface changes on identification reliability.

increased identification reliability to deep rolling. This increase is due to the higher roughness in turning and the higher stochastic component in grinding. As a result, more unique features are present in the high-frequency range, and thus the components can be identified with a higher degree of certainty. The results show that with a number of 21 matching features, an identification reliability of  $10^{20}$  is achieved for all manufacturing processes investigated.

In a final step, the turned samples are examined for mechanical wear. For this purpose, the samples are scratched with 500  $\mu\text{m}$  grit sandpaper. The extent to which a profile cross-section may change, so that identification of components is still possible, is examined. Figure 6 shows the comparison with a machined surface. It can be seen that with the removal of material by the abrasive paper, the feed grooves and tool sharpness are lost. The same behavior can be expected with wear due to frictional contact. However, the figure also shows that if a part of the original surface is still present, identification is possible. With a profile length of 1000 px, the tests have shown that identification is possible if 50 % of the profile is identical.

### 5. Discussion

Previous studies on marker-free component identification have dealt with plane surfaces produced by milling and grinding. The studies have shown that due the uniqueness of the features an exact alignment of the fingerprints is necessary for successful identification. This fact has been confirmed in this work, where for cylindrical grinding two profiles 500  $\mu\text{m}$  apart show very large changes. Plane surfaces have the advantage that their contour or prominent features such as holes can be used for alignment. To ensure that accurate positioning was possible for this work, a holder was constructed. By

drilling a hole in the sample, it was thus possible to realize the positioning. In addition to the already quantified processes, this paper demonstrates that turned and rolled surfaces can be identified by their unique features as well. For this purpose, in a first step, the continuous wavelet transformation together with the fingerprint was used to characterize the surface with a defined profile intersection. In this way, the unique features of the surface can be recognized. A backtracking from the features of the fingerprint to the emerging mechanisms was not done in this work. The result of the investigation was that for all three machining processes, the profile cut must be set in feed direction. With this knowledge, the parameters of the algorithm were optimized to achieve a high identification reliability for the three processes. With the parameters, the false-positive rate could then be determined using the probability model of Dragon et al. [5]. Due to the low proportion of stochastic features in the profile, deep rolling had the lowest identification reliability. The subsequent wear tests showed that a high percentage of the surface can be destroyed and yet identification is still possible. The exact percentage depends on the profile length and the number of stochastic features which are present. At the end of the investigations, it was determined that 50 features from the beginning must still be present for successful identification. The sample holder used in this work cannot be transferred to industry without significantly increasing the cycle time. For this reason, another way of capturing the surface has to be chosen. If it is not possible to identify the surface at prominent points, such as holes, the entire surface of the component must be measured first. For this purpose, a stepper motor including a drill chuck extended the measurement setup. The tool clamped in the drill chuck can then be rotated by a certain angle. All measurements for a specific angle are then combined. It is important that the samples are evenly illuminated so that an algorithm can combine the images. The dark field illumination used in this work does not allow such uniform illumination. It was found that the flat incidence of light allowed the distinctive features of the surface to be captured, but there was overexposure at the edges of the measurement. Therefore, a different type of exposure was investigated in a further series of tests. The light which is applied only from one side is a back light at a flat angle. This leads to a uniform exposure of the surface. This new type of exposure makes it possible to measure the surface area from several measurements. For the second measurement to identify the sample, only one measurement needs to be taken. This second measurement is now aligned with the mantle surface and the matching areas are compared.

## 6. Conclusion

Previous work has only dealt with the marker-free component identification of flat components. This work is the first to apply the approach to cylindrical components. By analyzing the surface to find a suitable profile cut and by adjusting the parameters of the identification algorithm, a false

positive rate of  $10^{-20}$  could be achieved in the investigations for the three manufacturing processes turning, grinding, and deep rolling. Due to the possibility of identifying cylindrical components without marking, complex active markings are no longer necessary. For cylindrical workpieces, this usually requires at least two additional production steps, which can now be saved and lead to an optimized production. Further studies should focus on the formation and back tracing of the features to individual mechanisms in order to gain a better understanding of the surface formation. In addition, wear tests show that identification is still possible despite surface changes. Therefore, the influence of coatings or heat treatments on the identification reliability will be investigated in further studies. In this way, it will be possible to trace components over several production steps in the future.

## Acknowledgments

The German Federation of Industrial Research Associations funded the presented investigations. We thank the foundation for their support and funding of the project Marker-Free Component identification under series conditions (21235 N/1).

## References

- [1] N. N.: VDMA-Studie Produktpiraterie 2020. VDMA Arbeitsgemeinschaft Produkt- und Know-how-Schutz. Frankfurt am Main, 2016
- [2] M. Liukkonen, T.-N. Tsai.: Toward decentralized intelligence in manufacturing: recent trends in automatic identification of things. The International Journal of Advanced Manufacturing Technology, Volume 87, Issue 9–12, Pages 2509–2531; 2016
- [3] Cowburn: Laser Surface Authentication - Biometrics for Brand Protection of Goods and Packaging. In: Kerry, J.; Butler, P. (Edit.): Smart Packaging Technologies for Fast Moving Consumer goods. Chichester: John Wiley & Sons; Pages 281-303; 2008
- [4] N. N.: Track & Trace per Fingerabdruck. Frauenhofer-Institut für Physikalische Messtechnik (IPM), Freiburg, 2017
- [5] R. Dragon; T. Mörke; B. Rosenhahn; J. Ostermann: Fingerprints for Machines - Characterization and Optical Identification of Grinding Imprints. DAGM Conference 2011, 33rd Annual Symposium of the German Association for Pattern Recognition, Frankfurt am Main; Pages 276-285; 2011
- [6] B. Breidenstein; B. Denkena; T. Mörke; R. Hockauf: Markierungsfreie Bauteil-Identifikation., wt Werkstatttechnik online, Issue 6, Pages 412 – 415; 2016
- [7] B. Breidenstein; T. Mörke; R. Hockauf; J. Ostermann; B. Spitschan: Component identification by means of unique topography features, Cyber Physical and Gentelligent Systems in Manufacturing and Life Cycle, Issue 1, Elsevier Fachverlag, Pages 12 – 28; 2017
- [8] Denkena, B.; Tönshoff, H.-K.: Spanen - Grundlagen, Berlin: Springer Verlag, 2011
- [9] Selvam, M.; Balakrishnanthe, K.: Study of machined surfaces roughness by random analysis, Wear, Volume 41, Pages 287–293, 1977
- [10] Liu, L.; Melkote, S.: Effect of plastic side flow on surface roughness in micro-turning process, International Journal of Machine Tool and Manufacture, Volume 46, Pages 1778- 1785, 2006
- [11] Grzesik, W.; Żak, K.: Modification of surface finish produced by hard turning using superfinishing and burnishing operations. Journal of Materials Processing Technology, Volume 212, Nr. 1, Pages 315–322, 2012
- [12] Denkena, B.; Abrão, A.; Krödel, A.; Meyer, K.: Analytic roughness prediction by deep rolling. Production Engineering, Volume 14, Number. 3, Pages 345-354, 2020
- [13] Fischler, Martin A; Robert C. Bolles: Random sample consensus: a paradigm for model fitting with applications to image analysis and automated cartography. Commun, ACM 24, Pages 381-395, 1981.